

Numerical homogenization of multiscale problems

Axel Målqvist¹

Fredrik Hellman (Uppsala) Anna Persson (Chalmers) Daniel Peterseim (Bonn)

Inaugural lecture

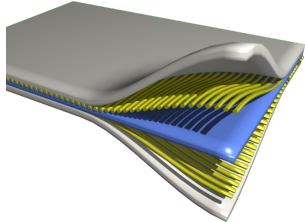
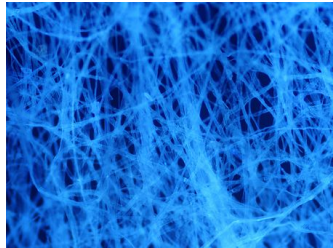
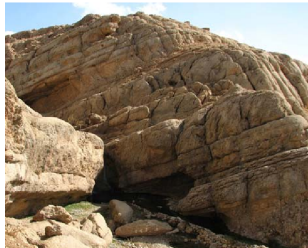
Department of Mathematical Sciences, Göteborg

2017-03-15

¹Chalmers University of Technology and University of Gothenburg

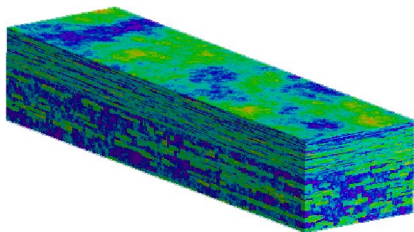
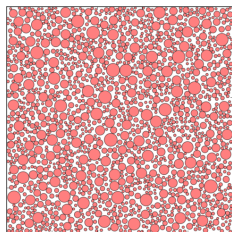


Multiscale materials



Multiscale problems

We consider applications such as



- ▷ composite materials ▷ flow in a porous medium

that require numerical solution of partial differential equations with rough data (module of elasticity, conductivity, or permeability).

Major challenge: Features on multiple non-separated scales.

Outline

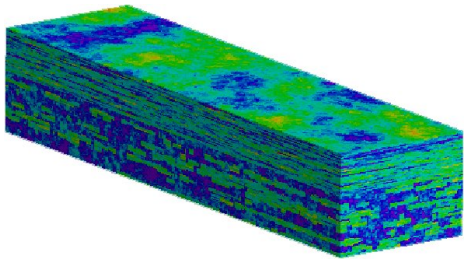
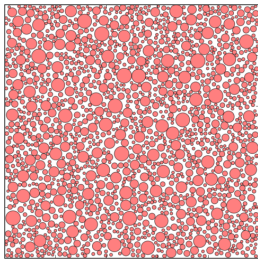
- ① **Elliptic problem: Homogenization and FEM**
- ② Introduction to LOD
- ③ High contrast data
- ④ Applications
- ⑤ Conclusions

Elliptic model problem

The Poisson equation

$$-\nabla \cdot \mathbf{A} \nabla u = f \quad \text{in } \Omega \qquad u = 0 \quad \text{on } \partial\Omega$$

with data $0 < \alpha \leq A \leq \beta < \infty$ and $f \in L^2(\Omega)$.



Homogenization of an elliptic model problem

The Poisson equation

$$-\nabla \cdot A \nabla u = f \quad \text{in } \Omega \quad u = 0 \quad \text{on } \partial\Omega$$

with data $0 < \alpha \leq A \leq \beta < \infty$ and $f \in L^2(\Omega)$.

Homogenization theory Let $A = A(x/\epsilon)$ be ϵ -periodic, and consider

$$-\nabla \cdot (A(x/\epsilon) \nabla u_\epsilon(x, x/\epsilon)) = f(x).$$

It can be shown that as $\epsilon \rightarrow 0$, $u_\epsilon \rightarrow v$ solves

$$-\nabla \cdot (A^* \nabla v(x)) = f(x),$$

- In 1D with no slow variation in A , $A^* = \frac{1}{\langle 1/A \rangle}$, i.e. the harmonic average.
- Otherwise A^* is computed by solving a cell problem.

Homogenization of an elliptic model problem

The Poisson equation

$$-\nabla \cdot \mathbf{A} \nabla u = f \quad \text{in } \Omega \quad u = 0 \quad \text{on } \partial\Omega$$

with data $0 < \alpha \leq A \leq \beta < \infty$ and $f \in L^2(\Omega)$.

Homogenization theory

- Requires $\epsilon \rightarrow 0$, i.e. very large scale separation.
- Requires periodic data.
- Complex geometry and boundary conditions are not covered by the theory.
- Numerical approaches inspired by homogenization theory (e.g. HMM and MsFEM) suffers from similar drawbacks.

Multiscale finite element method, (Hou & Wu), 1996.

Heterogeneous multiscale method, (Engquist & E), 2003.

Finite element method

The Poisson equation (weak form): $u \in V = H_0^1(\Omega)$ such that

$$a(u, v) := \int_{\Omega} (\textcolor{brown}{A} \nabla u) \cdot \nabla v \, dx = \int_{\Omega} f \cdot v \, dx \text{ for all } v \in V$$

with data $0 < \alpha \leq A \leq \beta < \infty$ and $f \in L^2(\Omega)$.

Finite element method

The Poisson equation (FE approximation): $u_h \in V_h \subset V$ such that

$$a(u_h, v) := \int_{\Omega} (\textcolor{brown}{A} \nabla u_h) \cdot \nabla v \, dx = \int_{\Omega} f \cdot v \, dx \text{ for all } v \in V_h$$

with data $0 < \alpha \leq A \leq \beta < \infty$ and $f \in L^2(\Omega)$.

Numerical error (piecewise linear continuous FE approximation)

- For solution $u \in H^2(\Omega)$ we have

$$\|u - u_h\| := \|A^{1/2} \nabla(u - u_h)\|_{L^2(\Omega)} \leq C\beta^{1/2} h \|D^2 u\|_{L^2(\Omega)} \sim C(\alpha, \beta, \textcolor{brown}{A}') h.$$

- The mesh size h has to resolve the variations in A , e.g. $h < \epsilon$ if A is ϵ -periodic.

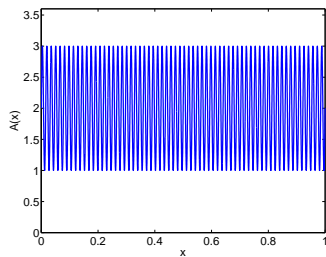
Finite element method

The Poisson equation (FE approximation): $u_h \in V_h \subset V$ such that

$$a(u_h, v) := \int_{\Omega} (\textcolor{brown}{A} \nabla u_h) \cdot \nabla v \, dx = \int_{\Omega} f \cdot v \, dx \text{ for all } v \in V_h$$

with data $0 < \alpha \leq A \leq \beta < \infty$ and $f \in L^2(\Omega)$.

Example (periodic coefficient): $A(x) = 2 + \sin(2\pi x/\varepsilon)$, $\varepsilon = 2^{-6}$, $f = 1$



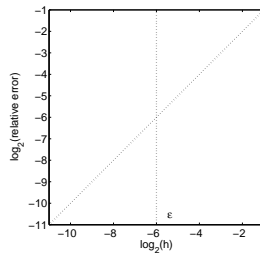
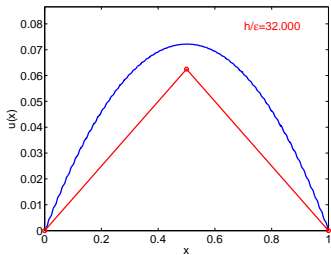
Finite element method

The Poisson equation (FE approximation): $u_h \in V_h \subset V$ such that

$$a(u_h, v) := \int_{\Omega} (\textcolor{brown}{A} \nabla u_h) \cdot \nabla v \, dx = \int_{\Omega} f \cdot v \, dx \text{ for all } v \in V_h$$

with data $0 < \alpha \leq A \leq \beta < \infty$ and $f \in L^2(\Omega)$.

Example (periodic coefficient): $A(x) = 2 + \sin(2\pi x/\varepsilon)$, $\varepsilon = 2^{-6}$, $f = 1$



solution and P1-FEM-approximation

$\log_2(H^1(\Omega) - \text{error})$ vs. $\log_2(h)$

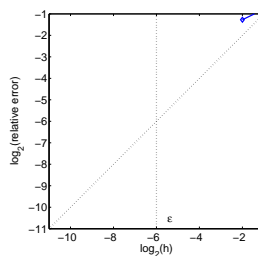
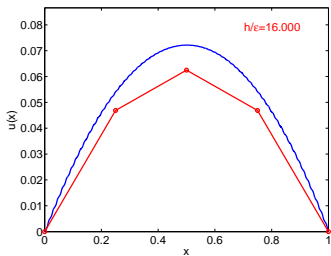
Finite element method

The Poisson equation (FE approximation): $u_h \in V_h \subset V$ such that

$$a(u_h, v) := \int_{\Omega} (\mathbf{A} \nabla u_h) \cdot \nabla v \, dx = \int_{\Omega} f \cdot v \, dx \text{ for all } v \in V_h$$

with data $0 < \alpha \leq A \leq \beta < \infty$ and $f \in L^2(\Omega)$.

Example (periodic coefficient): $A(x) = 2 + \sin(2\pi x/\varepsilon)$, $\varepsilon = 2^{-6}$, $f = 1$



solution and P1-FEM-approximation

$\log_2(H^1(\Omega) - \text{error})$ vs. $\log_2(h)$

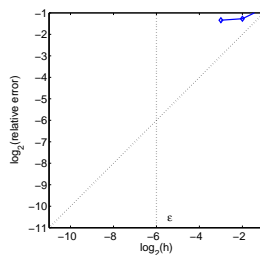
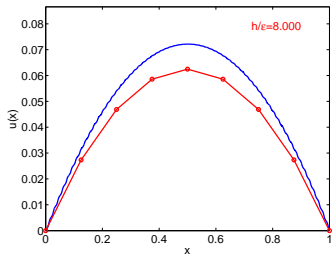
Finite element method

The Poisson equation (FE approximation): $u_h \in V_h \subset V$ such that

$$a(u_h, v) := \int_{\Omega} (\mathbf{A} \nabla u_h) \cdot \nabla v \, dx = \int_{\Omega} f \cdot v \, dx \text{ for all } v \in V_h$$

with data $0 < \alpha \leq A \leq \beta < \infty$ and $f \in L^2(\Omega)$.

Example (periodic coefficient): $A(x) = 2 + \sin(2\pi x/\varepsilon)$, $\varepsilon = 2^{-6}$, $f = 1$



solution and P1-FEM-approximation

$\log_2(H^1(\Omega) - \text{error})$ vs. $\log_2(h)$

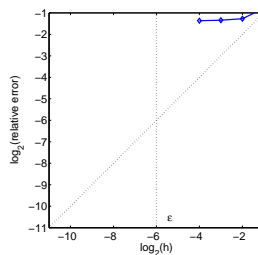
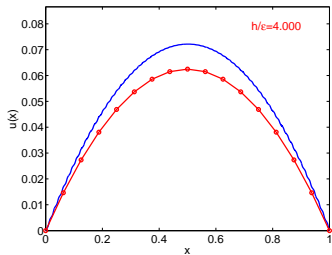
Finite element method

The Poisson equation (FE approximation): $u_h \in V_h \subset V$ such that

$$a(u_h, v) := \int_{\Omega} (\mathbf{A} \nabla u_h) \cdot \nabla v \, dx = \int_{\Omega} f \cdot v \, dx \text{ for all } v \in V_h$$

with data $0 < \alpha \leq A \leq \beta < \infty$ and $f \in L^2(\Omega)$.

Example (periodic coefficient): $A(x) = 2 + \sin(2\pi x/\varepsilon)$, $\varepsilon = 2^{-6}$, $f = 1$



solution and P1-FEM-approximation

$\log_2(H^1(\Omega) - \text{error})$ vs. $\log_2(h)$

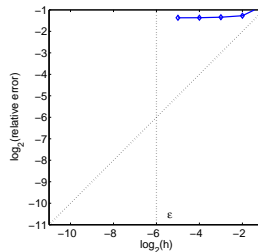
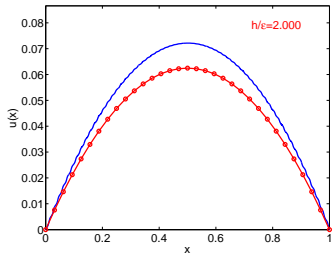
Finite element method

The Poisson equation (FE approximation): $u_h \in V_h \subset V$ such that

$$a(u_h, v) := \int_{\Omega} (\mathbf{A} \nabla u_h) \cdot \nabla v \, dx = \int_{\Omega} f \cdot v \, dx \text{ for all } v \in V_h$$

with data $0 < \alpha \leq A \leq \beta < \infty$ and $f \in L^2(\Omega)$.

Example (periodic coefficient): $A(x) = 2 + \sin(2\pi x/\varepsilon)$, $\varepsilon = 2^{-6}$, $f = 1$



solution and P1-FEM-approximation

$\log_2(H^1(\Omega) - \text{error})$ vs. $\log_2(h)$

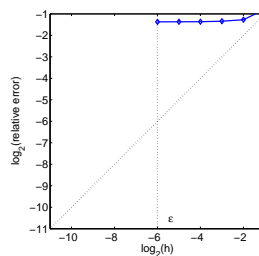
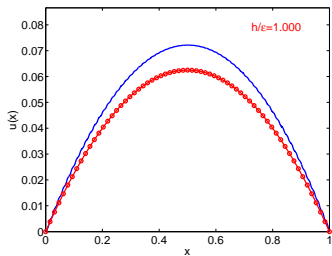
Finite element method

The Poisson equation (FE approximation): $u_h \in V_h \subset V$ such that

$$a(u_h, v) := \int_{\Omega} (\mathbf{A} \nabla u_h) \cdot \nabla v \, dx = \int_{\Omega} f \cdot v \, dx \text{ for all } v \in V_h$$

with data $0 < \alpha \leq A \leq \beta < \infty$ and $f \in L^2(\Omega)$.

Example (periodic coefficient): $A(x) = 2 + \sin(2\pi x/\varepsilon)$, $\varepsilon = 2^{-6}$, $f = 1$



solution and P1-FEM-approximation

$\log_2(H^1(\Omega) - \text{error})$ vs. $\log_2(h)$

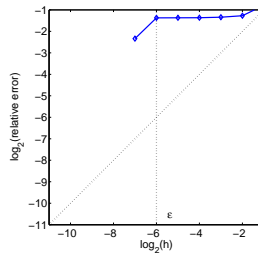
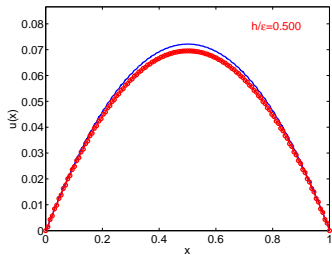
Finite element method

The Poisson equation (FE approximation): $u_h \in V_h \subset V$ such that

$$a(u_h, v) := \int_{\Omega} (\mathbf{A} \nabla u_h) \cdot \nabla v \, dx = \int_{\Omega} f \cdot v \, dx \text{ for all } v \in V_h$$

with data $0 < \alpha \leq A \leq \beta < \infty$ and $f \in L^2(\Omega)$.

Example (periodic coefficient): $A(x) = 2 + \sin(2\pi x/\varepsilon)$, $\varepsilon = 2^{-6}$, $f = 1$



solution and P1-FEM-approximation

$\log_2(H^1(\Omega) - \text{error})$ vs. $\log_2(h)$

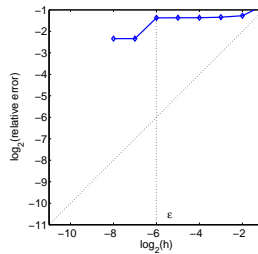
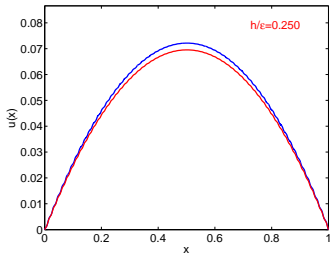
Finite element method

The Poisson equation (FE approximation): $u_h \in V_h \subset V$ such that

$$a(u_h, v) := \int_{\Omega} (\mathbf{A} \nabla u_h) \cdot \nabla v \, dx = \int_{\Omega} f \cdot v \, dx \text{ for all } v \in V_h$$

with data $0 < \alpha \leq A \leq \beta < \infty$ and $f \in L^2(\Omega)$.

Example (periodic coefficient): $A(x) = 2 + \sin(2\pi x/\varepsilon)$, $\varepsilon = 2^{-6}$, $f = 1$



solution and P1-FEM-approximation

$\log_2(H^1(\Omega) - \text{error})$ vs. $\log_2(h)$

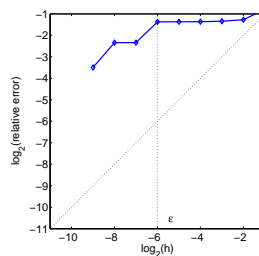
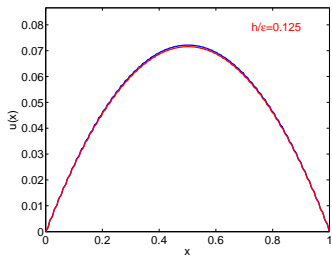
Finite element method

The Poisson equation (FE approximation): $u_h \in V_h \subset V$ such that

$$a(u_h, v) := \int_{\Omega} (\textcolor{brown}{A} \nabla u_h) \cdot \nabla v \, dx = \int_{\Omega} f \cdot v \, dx \text{ for all } v \in V_h$$

with data $0 < \alpha \leq A \leq \beta < \infty$ and $f \in L^2(\Omega)$.

Example (periodic coefficient): $A(x) = 2 + \sin(2\pi x/\varepsilon)$, $\varepsilon = 2^{-6}$, $f = 1$



solution and P1-FEM-approximation

$\log_2(H^1(\Omega) - \text{error})$ vs. $\log_2(h)$

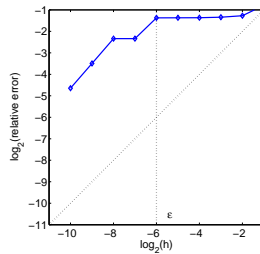
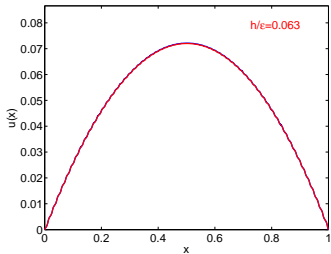
Finite element method

The Poisson equation (FE approximation): $u_h \in V_h \subset V$ such that

$$a(u_h, v) := \int_{\Omega} (\mathbf{A} \nabla u_h) \cdot \nabla v \, dx = \int_{\Omega} f \cdot v \, dx \text{ for all } v \in V_h$$

with data $0 < \alpha \leq A \leq \beta < \infty$ and $f \in L^2(\Omega)$.

Example (periodic coefficient): $A(x) = 2 + \sin(2\pi x/\varepsilon)$, $\varepsilon = 2^{-6}$, $f = 1$



solution and P1-FEM-approximation

$\log_2(H^1(\Omega) - \text{error})$ vs. $\log_2(h)$

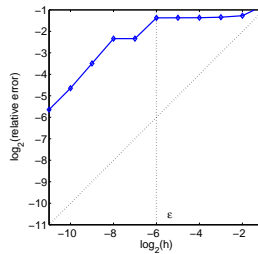
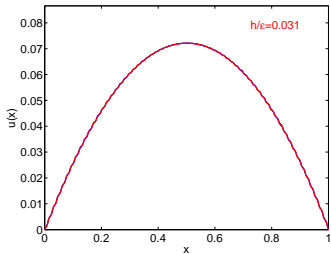
Finite element method

The Poisson equation (FE approximation): $u_h \in V_h \subset V$ such that

$$a(u_h, v) := \int_{\Omega} (\mathbf{A} \nabla u_h) \cdot \nabla v \, dx = \int_{\Omega} f \cdot v \, dx \text{ for all } v \in V_h$$

with data $0 < \alpha \leq A \leq \beta < \infty$ and $f \in L^2(\Omega)$.

Example (periodic coefficient): $A(x) = 2 + \sin(2\pi x/\varepsilon)$, $\varepsilon = 2^{-6}$, $f = 1$



solution and P1-FEM-approximation

$\log_2(H^1(\Omega) - \text{error})$ vs. $\log_2(h)$

New numerical approach

Objectives:

- Find a subspace of $V_H^{\text{ms}} \subset V_h$ for which the Galerkin approximation fulfills

$$\|u_h - u_H^{\text{ms}}\| \leq C(\alpha, \beta)H \approx C(\alpha, \beta, \mathbf{A}')h,$$

but with $\dim(V_H^{\text{ms}}) \ll \dim(V_h)$.

- Show that a basis for V_H^{ms} can be constructed by local parallel computations.
- Demonstrate efficiency for applications where V_H^{ms} is reused (eigenvalue, time dependent, semi-linear, systems).

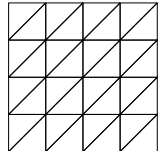
Variational multiscale method, (Hughes), 1995

Outline

- ① Elliptic problem: Homogenization and FEM
- ② **Introduction to LOD**
- ③ High contrast data
- ④ Applications
- ⑤ Conclusions

Multiscale decomposition

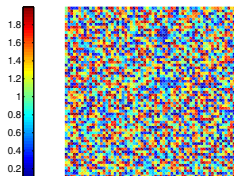
- (coarse) FE mesh \mathcal{T} with parameter $H > h$
- P1-FE space $V_H := \{v \in V \mid \forall T \in \mathcal{T}, v|_T \in P_1(T)\}$
- $\mathfrak{I}_{\mathcal{T}} : V \rightarrow V_H$ some interpolation operator



Decomposition

$$V = V_H \oplus V^f \quad \text{with } V^f := \text{kernel } \mathfrak{I}_{\mathcal{T}} = \{v \in V \mid \mathfrak{I}_{\mathcal{T}} v = 0\}$$

Example:



rough coefficient

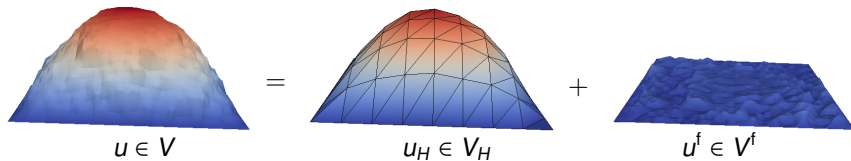
Multiscale decomposition

- (coarse) FE mesh \mathcal{T} with parameter $H > h$
- P1-FE space $V_H := \{v \in V \mid \forall T \in \mathcal{T}, v|_T \in P_1(T)\}$
- $\mathfrak{I}_{\mathcal{T}} : V \rightarrow V_H$ some interpolation operator

Decomposition

$$V = V_H \oplus V^f \quad \text{with } V^f := \text{kernel } \mathfrak{I}_{\mathcal{T}} = \{v \in V \mid \mathfrak{I}_{\mathcal{T}} v = 0\}$$

Example:



Orthogonalization

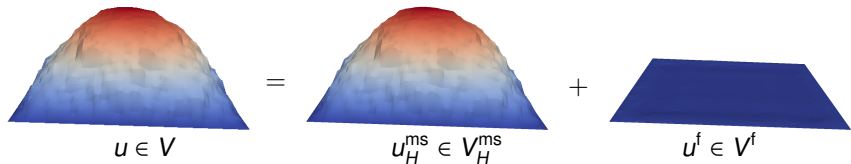
- For each $v \in V$ define finescale projection $Qv \in V^f$ by

$$a(Qv, w) = a(v, w) \quad \text{for all } w \in V^f$$

a -Orthogonal Decomposition

$$V = V_H^{\text{ms}} \oplus V^f \quad \text{with } V_H^{\text{ms}} := (V_H - QV_H)$$

Example:



Ideal multiscale representation

Given the space V_H^{ms} we construct a Galerkin approximation:

Ideal method

Find $u_H^{\text{ms}} \in V_H^{\text{ms}}$ such that

$$a(u_H^{\text{ms}}, v) = (f, v), \quad \forall v \in V_H^{\text{ms}}.$$

We have that $u - u_H^{\text{ms}} = u_f \in V^f$ since u_H^{ms} is the a -orthogonal projection of u onto V_H^{ms} . Therefore

$$\|u_f\|^2 = a(u, u_f) = (f, u_f) = (f, u_f - \mathfrak{I}_{\mathcal{T}} u_f) \leq \frac{C_{\mathfrak{I}_{\mathcal{T}}}}{\alpha^{1/2}} \|Hf\|_{L^2(\Omega)} \|u_f\|.$$

For V_H^{ms} to be useful we need a discrete local basis.

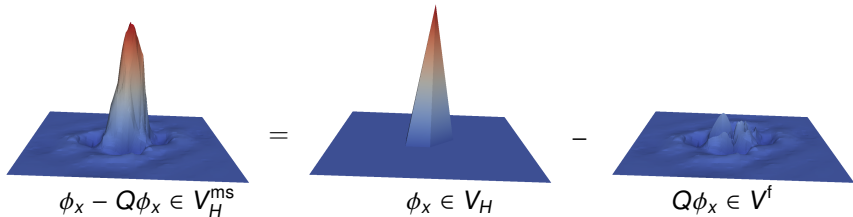
Modified nodal basis

- \mathcal{N} denotes set of interior vertices of \mathcal{T}
- $\phi_x \in V_H$ denotes classical nodal basis function ($x \in \mathcal{N}$)
- $Q\phi_x \in V^f$ denotes the finescale correction of ϕ_x ($x \in \mathcal{N}$)

Ideal multiscale FE space

$$V_H^{\text{ms}} = \text{span} \{ \phi_x - Q\phi_x \mid x \in \mathcal{N} \}$$

Example



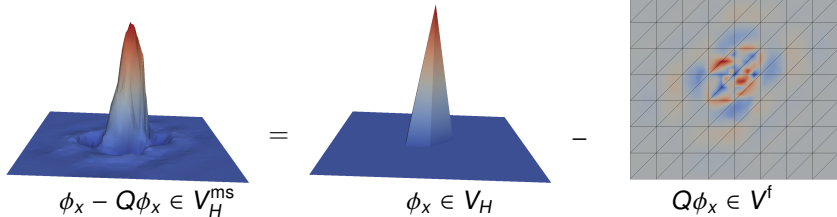
Modified nodal basis

- \mathcal{N} denotes set of interior vertices of \mathcal{T}
- $\phi_x \in V_H$ denotes classical nodal basis function ($x \in \mathcal{N}$)
- $Q\phi_x \in V^f$ denotes the finescale correction of ϕ_x ($x \in \mathcal{N}$)

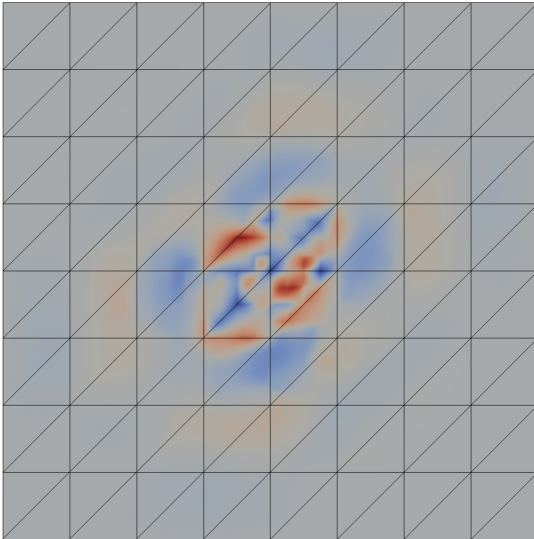
Ideal multiscale FE space

$$V_H^{\text{ms}} = \text{span} \{ \phi_x - Q\phi_x \mid x \in \mathcal{N} \}$$

Example

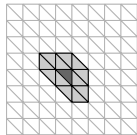
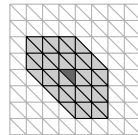


Modified nodal basis



Localization

- Define nodal patches of ℓ -th order $\omega_{T,\ell}$ about $T \in \mathcal{T}$

 $\omega_{T,1}$  $\omega_{T,2}$

- Correctors $Q_\ell^T \phi_x \in V^f(\omega_{T,\ell}) := \{v \in V^f \mid v|_{\Omega \setminus \omega_{T,\ell}} = 0\}$ solve

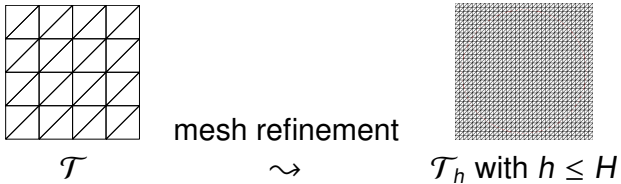
$$a(Q_\ell^T \phi_x, w) = \int_T A \nabla \phi_x \cdot \nabla w \, dx \quad \text{for all } w \in V^f(\omega_{T,\ell})$$

Localized multiscale FE spaces

$$V_{H,\ell}^{\text{ms}} = \text{span}\{\phi_x - \sum_{T \in \mathcal{T}} Q_\ell^T \phi_x \mid x \in \mathcal{N}\}$$

Fine scale discretization

- Finescale mesh



- Reference FE space

$$V_h := \{v \in V \mid \forall T \in \mathcal{T}(\Omega), v|_T \in P_1(T)\}$$

- Reference FE solution $u_h \in V_h$ solves

$$a(u_h, v) = (f, v) \quad \text{for all } v \in V_h$$

- Fully discrete correctors $Q_{\ell,h}^T \phi_x \in V_h^f(\omega_{T,\ell}) := V^f(\omega_{T,\ell}) \cap V_h$:

$$a(Q_{\ell,h}^T \phi_x, w) = (A \nabla \phi_x, \nabla w)_T \quad \text{for all } w \in V_h^f(\omega_{T,\ell})$$

Localized Orthogonal Decomposition (LOD)

Fully discrete multiscale FE spaces

$$V_{H,\ell}^{\text{ms},h} = \text{span}\{\phi_x - \sum_{T \in \mathcal{T}} Q_{\ell,h}^T \phi_x \mid x \in \mathcal{N}\}$$

Fully discrete multiscale approximation $u_{H,\ell}^{\text{ms},h} \in V_{H,\ell}^{\text{ms},h}$

$$a(u_{H,\ell}^{\text{ms},h}, v) = (f, v) \quad \text{for all } v \in V_{H,\ell}^{\text{ms},h}$$

Remarks:

- $\dim V_{H,\ell}^{\text{ms},h} = |\mathcal{N}| = \dim V_H$
- The basis functions have local support, with overlap depending on ℓ , and are independent.

A priori error analysis

Lemma (Truncation error)

$$\|Q_h v_H - Q_{\ell,h} v_H\| \leq C_1 \gamma^\ell \|Q_h v_H\|, \quad \forall v_h \in V_H$$

$C_1 < \infty$ and $\gamma < 1$ depends on β/α but not A' .

By choosing $\ell = C_2 \log(H^{-1})$ with appropriate C_2 we guarantee that the truncation leads to a higher order perturbation:

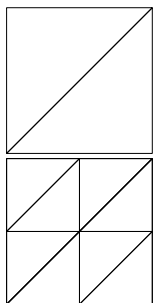
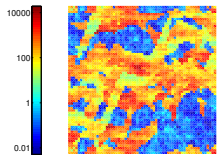
Theorem (A priori error bound)

$$\|u_h - u_{H,\ell}^{\text{ms},h}\| \leq C(\alpha, \beta) H,$$

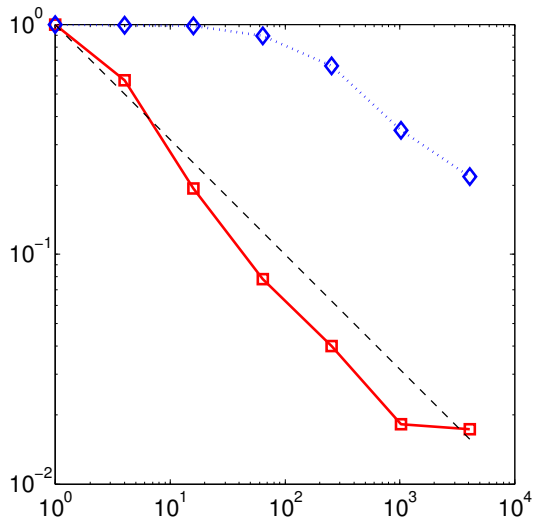
with C independent of A' .

M. & Peterseim, Localization of elliptic multiscale problems, 2014.

Numerical experiment: Poisson's equation

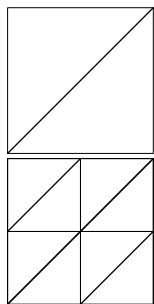
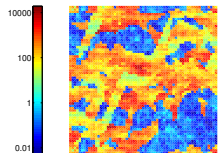


$$H = 2^{-1}, 2^{-2}, \dots, 2^{-7}$$
$$h = 2^{-9}, \ell = \log(1/H)$$

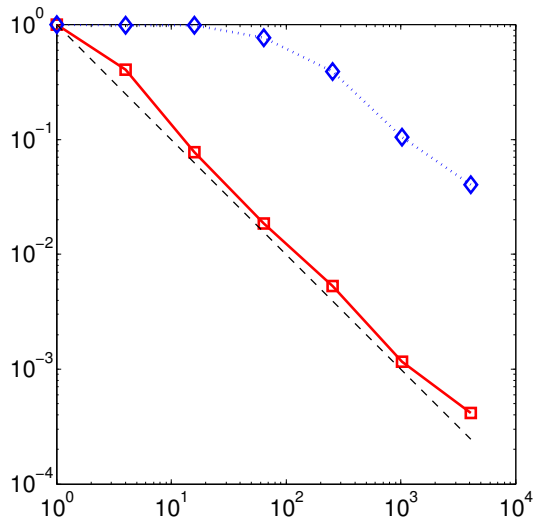


$\| \|u_h - u_{H,\ell}^{\text{ms},h}\| \|$ vs. #dof

Numerical experiment: Poisson's equation

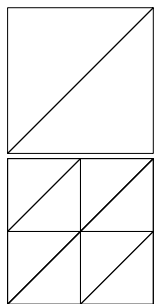
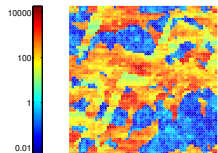


$$H = 2^{-1}, 2^{-2}, \dots, 2^{-7}$$
$$h = 2^{-9}, \ell = \log(1/H)$$

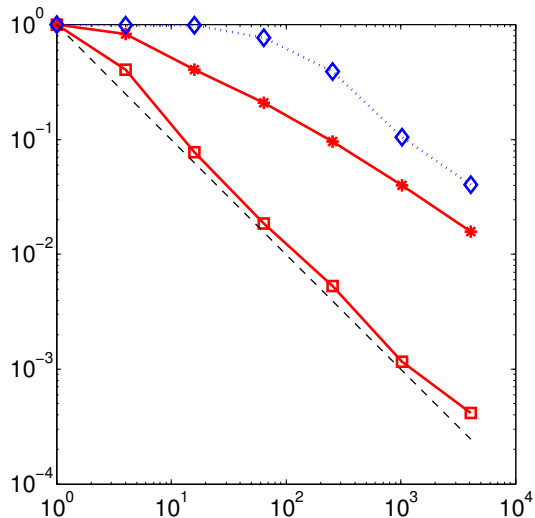


$\|u_h - u_{H,\ell}^{\text{ms},h}\|$ vs. #dof

Numerical experiment: Poisson's equation



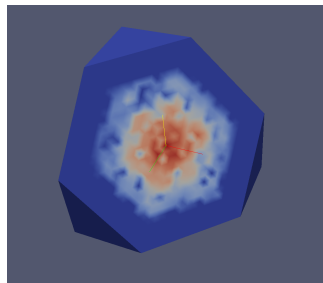
$$H = 2^{-1}, 2^{-2}, \dots, 2^{-7}$$
$$h = 2^{-9}, \ell = \log(1/H)$$



$\|u_h - \mathfrak{I}_T u_{H,\ell}^{\text{ms},h}\|$ vs. #dof

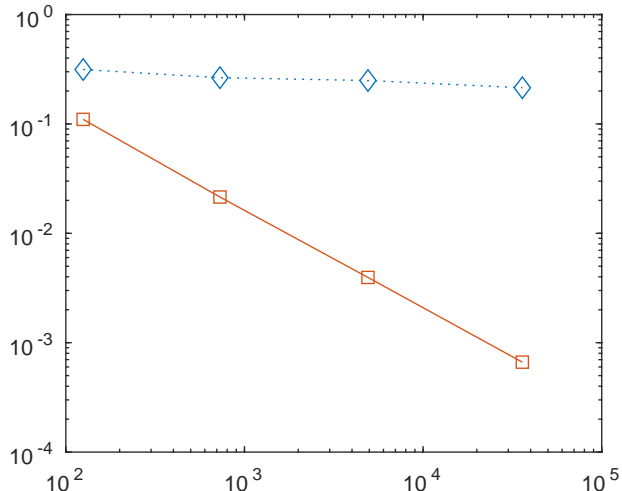
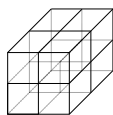
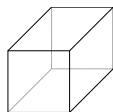
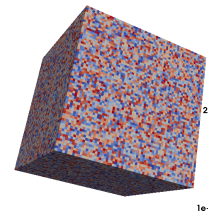
3D implementation in python

- Trilinear shape functions on cubes.
- Petrov-Galerkin formulation reduces communication, Elfversson et.al. Numer. Math. 2016.
- Storage of all basis function is not needed. The full solution can be recomputed (at a lower cost) once $\mathfrak{I}_{\mathcal{T}} u_{H,\ell}^{\text{ms},h}$ is computed.



Corrector function $Q^T \phi_x$, implementation by Fredrik Hellman.

Numerical experiment: Poisson's equation 3D

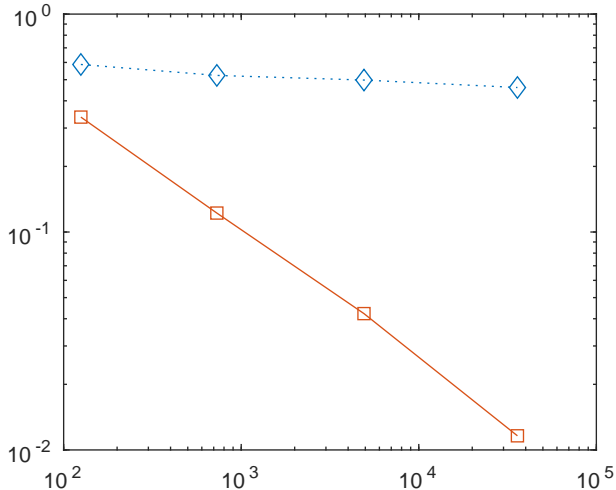
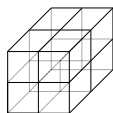
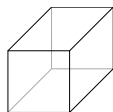
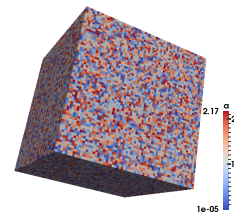


$$H = 2^{-2}, 2^{-3}, 2^{-4}, 2^{-5}$$

$$h = 2^{-6}, \ell = \log(1/H)$$

$\|u_h - u_{H,\ell}^{ms,h}\|$ vs. #dof

Numerical experiment: Poisson's equation 3D

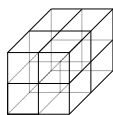
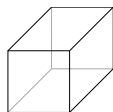
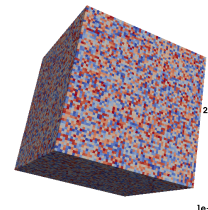


$$H = 2^{-2}, 2^{-3}, 2^{-4}, 2^{-5}$$

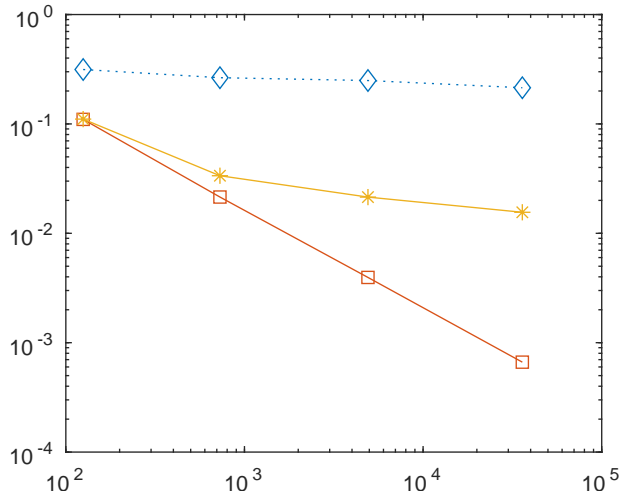
$$h = 2^{-6}, \ell = \log(1/H)$$

$\|u_h - u_{H,\ell}^{ms,h}\|$ vs. #dof

Numerical experiment: Poisson's equation 3D



$$H = 2^{-2}, 2^{-3}, 2^{-4}, 2^{-5}$$
$$h = 2^{-6}, \ell = \log(1/H)$$



$\|u_h - \mathfrak{I}_\tau u_{H,\ell}^{ms,h}\|$ vs. #dof

Outline

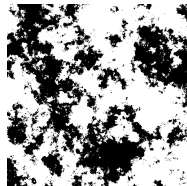
- ① Elliptic problem: Homogenization and FEM
- ② Introduction to LOD
- ③ **High contrast data**
- ④ Applications
- ⑤ Conclusions

High contrast data

Poisson equation:

$$-\nabla \cdot A \nabla u = f \quad \text{in } \Omega \quad u = 0 \quad \text{on } \partial\Omega.$$

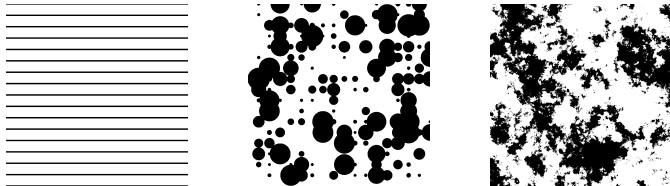
$A = 1$ in Ω_1 (black), $A = \alpha$ in Ω_α , $\alpha \ll 1$, and $f = \chi_{[1/4,3/4]^2}$.



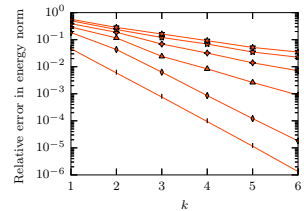
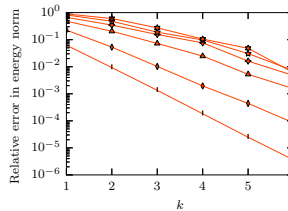
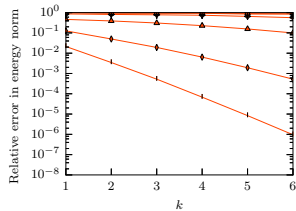
- High contrast data with channels leads to non-local behaviour.
- The decay rate of the basis functions determines the accuracy of LOD.
- The choice of interpolant $\mathfrak{I}_T v = \sum_{x \in N} \bar{v}_{\omega_x} \phi_x$ affects the decay.

Numerical example: High contrast

High contrast data Three examples: $H = 2^{-4}$, $h = 2^{-10}$,



We let $\alpha = 10^{-1}, \dots, 10^{-6}$ and plot $\|u_h - u_{H,k}^{\text{ms},h}\|$ vs. k , with $\mathfrak{I}_{\mathcal{T}}^{SZ}$,



Scott-Zhang type interpolation

Nodal variables:

Let $x \in \mathcal{N}$ be nodes of \mathcal{T} and $\sigma_x \subset \Omega$ associated domains. We define a $L^2(\sigma_x)$ -dual basis $\psi_x \in V_H$ fulfilling,

$$\int_{\sigma_x} \psi_x \phi_y = \delta_{xy}.$$

Let the nodal variable $N_x(v) = \int_{\sigma_x} \psi_x v$ and,

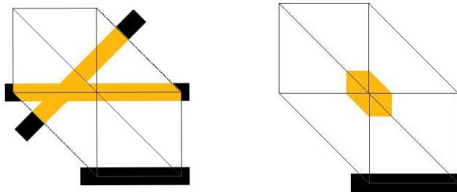
$$\mathfrak{I}_{\mathcal{T}}^\sigma v = \sum_{x \in \mathcal{N}} N_x(v) \phi_x.$$

- σ_x does not need to be full elements T or vertex patches $U_1(x)$.
- The stability of $|N_x(v)| \leq \|\psi\|_{L^2(\sigma_x)} \|v\|_{L^2(\sigma_x)}$ depends on the size and shape of σ_x and its distance to x .

Geometry dependent interpolation

Selection of σ_x :

By letting $\sigma_x \subset \Omega_1$ (frequently enough) we guarantee decay, i.e. nodes in high conductivity channels are needed.



Let $U_1(x)$ be the vertex patch at node x .

- Type I node: for $x \in \Omega_1$ let $\sigma_x \subset U_1(x) \cap \Omega_1$, connected, and chosen so $\inf_{q \in \mathbb{R}} \|v - q\|_{L^2(\sigma_x)} \leq CH \|\nabla v\|_{L^2(\sigma_x)}$ holds (Poincaré).
- Type II node: for $x \in \Omega_\alpha$ let $\sigma_x = U_\delta(x)$, $0 < \delta \leq 1$,

Weighted Poincaré inequality and decay

The following weighted Poincaré inequality holds:

$$\|A^{1/2}v_f\|_{L^2(\mathcal{T})} \leq CH \|A^{1/2}\nabla v_f\|_{L^2(U_1(\mathcal{T}))}, \quad \forall v_f \in V^f = \ker(\mathfrak{J}_{\mathcal{T}}^{\sigma}).$$

This is used to prove contrast independent decay.

Theorem

With $\delta < 1/2$ we have,

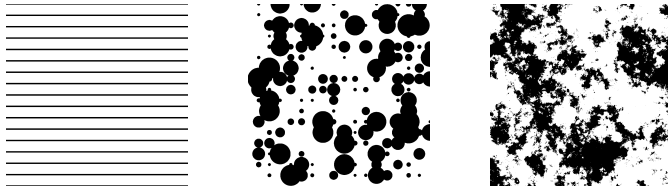
$$\|A^{1/2}\nabla Q^T v_H\|_{\Omega \setminus U_k(\mathcal{T})} \leq C\gamma^k \|A^{1/2}\nabla Q^T v_H\|_{L^2(\Omega)},$$

where C and γ are independent of β/α .

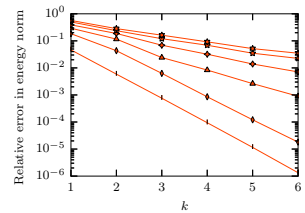
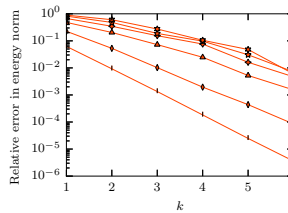
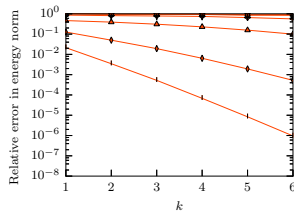
Hellman & M. Contrast independent localization of multiscale problems,
arXiv

Numerical example: High contrast

High contrast data Three examples: $H = 2^{-4}$, $h = 2^{-10}$,



We let $\alpha = 10^{-1}, \dots, 10^{-6}$ and plot $\|u_h - u_{H,k}^{\text{ms},h}\|$ vs. k with $\mathfrak{I}_{\mathcal{T}}^{\text{SZ}}$,

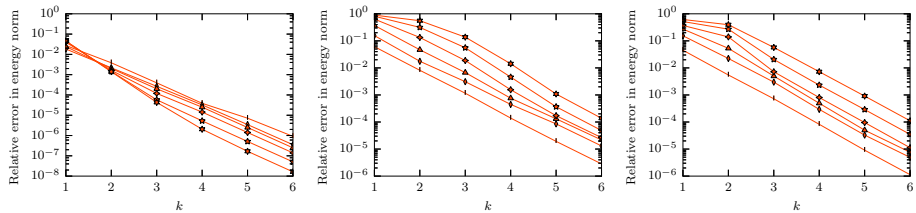


Numerical example: High contrast

High contrast data Three examples: $H = 2^{-4}$, $h = 2^{-10}$,



We let $\alpha = 10^{-1}, \dots, 10^{-6}$ and plot $\|u_h - u_{H,k}^{\text{ms},h}\|$ vs. k with \mathfrak{I}_T^σ ,



Outline

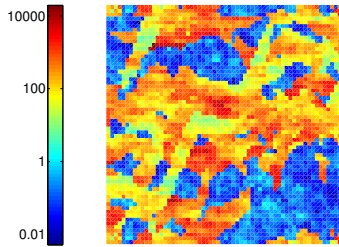
- ① Elliptic problem: Homogenization and FEM
- ② Introduction to LOD
- ③ High contrast data
- ④ **Applications**
- ⑤ Conclusions

Model multiscale eigenvalue problem

Prototypical self-adjoint eigenvalue problem

$$-\nabla \cdot \mathbf{A} \nabla u = \lambda u \quad \text{in } \Omega \quad u = 0 \quad \text{on } \partial\Omega$$

with data $0 < \alpha \leq A \leq \beta < \infty$

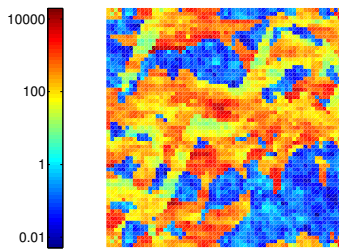


Model multiscale eigenvalue problem

Prototypical self-adjoint eigenvalue problem (variational form): find $u \in V := H_0^1(\Omega)$ and $\lambda \in \mathbb{R}$ such that

$$a(u, v) := \int_{\Omega} (\mathbf{A} \nabla u) \cdot \nabla v \, dx = \lambda \int_{\Omega} u \cdot v \, dx \text{ for all } v \in V$$

with data $0 < \alpha \leq A \leq \beta < \infty$

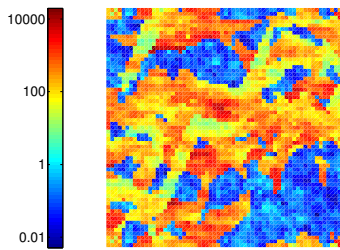


Model multiscale eigenvalue problem

Prototypical self-adjoint eigenvalue problem (FE approximation):
 $u_h \in V_h \subset V$ and $\lambda_h \in \mathbb{R}$ such that

$$a(u_h, v) := \int_{\Omega} (\mathbf{A} \nabla u_h) \cdot \nabla v \, dx = \lambda_h \int_{\Omega} u_h \cdot v \, dx \text{ for all } v \in V_h$$

with data $0 < \alpha \leq A \leq \beta < \infty$



Model multiscale eigenvalue problem

Prototypical self-adjoint eigenvalue problem (FE approximation):
 $u_h \in V_h \subset V$ and $\lambda_h \in \mathbb{R}$ such that

$$a(u_h, v) := \int_{\Omega} (\mathbf{A} \nabla u_h) \cdot \nabla v \, dx = \lambda_h \int_{\Omega} u_h \cdot v \, dx \text{ for all } v \in V_h$$

with data $0 < \alpha \leq A \leq \beta < \infty$

Numerical error (piecewise linear continuous FE approximation)

- For an eigenpair $(u^{(k)}, \lambda^{(k)})$ with $u^{(k)} \in H^2(\Omega)$ it holds

$$\lambda^{(k)} \leq \lambda_h^{(k)} \leq \lambda^{(k)} + C(\alpha, \beta, \mathbf{A}', k) h^2,$$

$$\|u^{(k)} - u_h^{(k)}\| := \|\mathbf{A}^{1/2} \nabla (u^{(k)} - u_h^{(k)})\|_{L^2(\Omega)} \leq C(\alpha, \beta, \mathbf{A}', k) h.$$

- The mesh size h has to resolve the variations in A , e.g. $h < \epsilon$ if A is periodic.

LOD approximation

LOD: Find $u_{H,\ell}^{\text{ms},h} \in V_{H,\ell}^{\text{ms},h}$, $\lambda_{H,\ell}^{\text{ms},h} \in \mathbb{R}$

$$a(u_{H,\ell}^{\text{ms},h}, v) = \lambda_{H,\ell}^{\text{ms},h}(u_{H,\ell}^{\text{ms},h}, v) \quad \text{for all } v \in V_{H,\ell}^{\text{ms},h}$$

Theorem

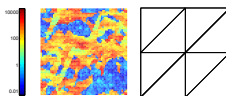
$$\lambda_h^{(k)} \leq \lambda_{H,\ell}^{\text{ms},h,(k)} \leq \lambda_h^{(k)} + CH^4,$$

$$\|u_h^{(k)} - u_{H,\ell}^{\text{ms},h,(k)}\| \leq CH^2,$$

with C independent of A' and the regularity of the eigenfunctions and (λ_h, u_h) is the reference solution.

M. & Peterseim, Computation of eigenvalues by nume. upscaling, 2015.

Numerical example: eigenvalues



k	$\lambda_h^{(k)}$	$e^{(k)}(1/2\sqrt{2})$	$e^{(k)}(1/4\sqrt{2})$	$e^{(k)}(1/8\sqrt{2})$	$e^{(k)}(1/16\sqrt{2})$
1	21.4144522	5.472755371	0.237181706	0.010328293	0.000781683
2	40.9134676	-	0.649080539	0.032761482	0.002447049
3	44.1561133	-	1.687388874	0.097540102	0.004131422
4	60.8278691	-	1.648439518	0.028076168	0.002079812
5	65.6962136	-	2.071005692	0.247424446	0.006569640
6	70.1273082	-	4.265936007	0.232458016	0.016551520
7	82.2960238	-	3.632888104	0.355050163	0.013987920
8	92.8677605	-	6.850048057	0.377881216	0.049841235
9	99.6061234	-	10.305084010	0.469770376	0.026027378
10	109.1543283	-	-	0.476741452	0.005606426
11	129.3741945	-	-	0.505888044	0.062382302
12	138.2164330	-	-	0.554736550	0.039487317
13	141.5464639	-	-	0.540480876	0.043935515
14	145.7469718	-	-	0.765411709	0.034249528
15	152.6283573	-	-	0.712383825	0.024716759
16	155.2965039	-	-	0.761104705	0.026228034
17	158.2610708	-	-	0.749058367	0.091826207
18	164.1452194	-	-	0.840736127	0.118353184
19	171.1756923	-	-	0.946719951	0.111314058
20	179.3917590	-	-	0.928617606	0.119627862

Table: Errors $e^{(k)}(H) =: \frac{\lambda_H^{\text{ms},(k)} - \lambda_h^{(k)}}{\lambda_h^{(k)}}$ and $h = 2^{-7} \sqrt{2}$.

Parabolic equations

The parabolic problem: Find $u \in V$ such that

$$(\dot{u}, v) + (A \nabla u, \nabla v) = (f(t), v), \quad \forall v \in V, \quad t > 0$$

and $u(0) = u_0 \in L^2(\Omega)$. We assume A to be independent of t .

FE Backward Euler: Find $u_h^n \in V_h$ such that

$$(\bar{\partial}_t u_h^n, v) + a(u_h^n, v) = (f^n, v), \quad \forall v \in V_h,$$

and $u_h^0 \in V_h$ some approximation of u_0 .

LOD: Find $(u_H^{\text{ms}})^n \in V_{H,\ell}^{\text{ms},h}$ such that

$$(\bar{\partial}_t (u_H^{\text{ms}})^n, v) + a((u_H^{\text{ms}})^n, v) = (f^n, v), \quad \forall v \in V_{H,\ell}^{\text{ms},h},$$

and $(u_H^{\text{ms}})^0 \in V_{H,\ell}^{\text{ms},h}$ some approximation of u_0 .

Parabolic equations

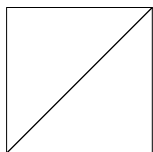
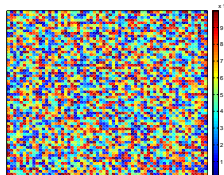
Theorem

$$\|u_h^n - (u_H^{\text{ms}})^n\|_{L^2(\Omega)} \leq C(1 + \log(\frac{t_n}{\tau}))H^2(t_n^{-1}\|u_h^0\|_{L^2(\Omega)} + \|f\|_{W^{1,\infty}(L^2(\Omega))})$$

with C independent of A' .

- The analysis uses classic a priori error estimation techniques and the elliptic results.
- The term t_n^{-1} appears also in $u - u_h$ bounds if $u_0 \in L^2(\Omega)$. The log term can be avoided if $f(t) \in H_0^1(\Omega)$.
- The case $f = f(u)$ can also be treated, under certain growth conditions on $f'(u)$ and $f''(u)$.
- The case $A = A(t)$ or $A = A(u)$ is not covered and would require updates of $V_{H,\ell}^{\text{ms},h}$.

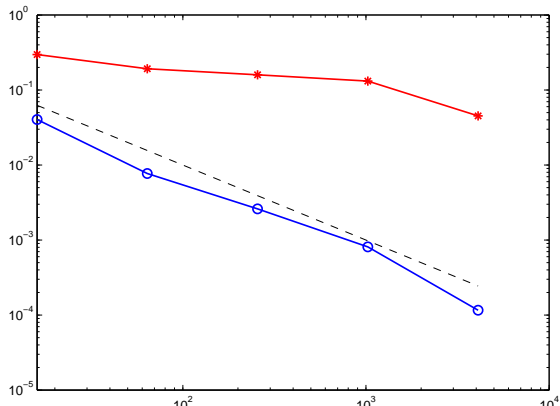
Numerical experiment: The heat equation



$$H = 2^{-1}, 2^{-2}, \dots, 2^{-6}$$

$$h = 2^{-7}, \ell = \log(1/H), u_0 = 1,$$

$$T = 1, \tau = 0.001$$



$\|u_h^n - (u_H^{ms})^n\|$ vs. #dof

M.& Persson, *Multiscale techniques for parabolic problems*, arXiv
1504.08140.

More applications

Stationary/eigenvalue problems

- Semilinear, (Henning, M., Peterseim), 2014.
- Gross-Pitaevskii, (Henning, M., Peterseim), 2014.
- Helmholtz, (Gallistl & Peterseim), 2015.
- Reduced basis, (Abdulle & Henning), 2015.
- Elasticity, (Henning & Persson), 2016.
- High contrast, (Peterseim & Scheichl), 2016.
- Helmholtz, (Ohlberger & Verfürth), 2017.
- Iterative solvers, (Kornhuber & Yserentant), 2017.

Time-dependent problems

- Thermoelasticity, (M. & Persson), 2017.
- Wave equation, (Abdulle & Henning), 2017.
- Two phase flow, (Hellman & M.), ongoing

Outline

- ① Elliptic problem: Homogenization and FEM
- ② Introduction to LOD
- ③ High contrast data
- ④ Applications
- ⑤ **Conclusions**

Conclusion and outlook

- By LOD we compute an effective stiffness matrix on a coarse scale. (numerical homogenization)
- Rapidly varying diffusion of low contrast is well understood.
- Recent development in high contrast problems which is a great challenge for any method.
- Great reduction in computational cost when the basis is reused (load cases, eigenvalues, time dependent, non-linear, control).
- Future challenges: random diffusion, quasi-linear problems, efficient implementation, nearly periodic problems.

Thank you for your attention!